Astron. Astrophys. 334, L13–L16 (1998)

ASTRONOMY AND ASTROPHYSICS

LETTER

Letter to the Editor

The cosmic X-ray background spectrum observed with ROSAT and ASCA

T. Miyaji[1,2], Y. Ishisaki[3], Y. Ogasaka[4,5], Y. Ueda[5], M.J. Freyberg[2], G. Hasinger[1], and Y. Tanaka[2]

[1] Astrophysikalisches Institut Potsdam, An der Sternwarte 16, D-14482 Potsdam, Germany
[2] Max-Planck-Institut für Extraterrestrische Physik, D-85740 Garching bei München, Germany
[3] Tokyo Metropolitan University, 1-1 Minami-Osawa, Hachioji, 192-03, Japan
[4] Code 662, NASA Goddard Space Flight Center, MD 20771, USA
[5] The Institute of Space and Astronautical Sciences, 3-1-1, Yoshinodai, Sagamihara, 229, Japan

Received 16 September 1997 / Accepted 20 March 1998

Abstract. We have made a series of joint spectral fits for two blank fields, the Lockman Hole and the Lynx-3A field, where a significant amount of both *ASCA* and *ROSAT* PSPC data exist after thorough screenings. The *ASCA* SIS, GIS and *ROSAT* PSPC spectra from these fields have been fitted simultaneously. Comparison at $E > 1$ keV shows general agreement within 10% in the Lockman Hole data and a $20-30\%$ disagreement in the Lynx-3A data, indicating remaining observation-dependent systematic problems. In both cases, satisfactory fits have been found for the overall 0.1–10 keV spectrum with an extragalactic power-law component (or a broken power-law component with steepening at $E < 1$ keV), a hard thermal component with plasma temperature of $kT^{\rm h} \approx 0.14$ keV and a soft thermal component $kT^{\rm s} \approx 0.07$ keV.

Key words: ISM: bubbles – galaxy: halo – cosmology: diffuse radiation – X-rays: general

1. Introduction

The global spectrum of the cosmic X-ray background is a primary piece of information for understanding its origin. The 3-50 keV CXRB spectrum observed with HEAO-1 A2 can be well described by a $kT = 40$ keV thin thermal plasma-like spectral shape (Marshall et al. 1980; Boldt 1987), which can be approximated by a power-law with a photon index of $\Gamma = 1.4$ in $E \lesssim 10$ keV. *BBXRT* (Jahoda et al. 1992) and *ASCA* (Gendreau et al. 1995; Ishisaki et al. 1998) measurements show that this power-law component extends down to 1 keV, below which an excess is observed.

A number of authors report *ROSAT* measurements in the 0.5-2 keV band (e.g. Hasinger 1992; Georgantopoulos et al. 1996) and show about 30% larger flux than the Gendreau et al.'s (1995) *ASCA* SIS result at 1 keV, with different slopes (see Hasinger 1996 for review). The disagreement may be contributed by the differences in the position/solid angle of the measured sky, problems arising from incomplete modelings, and/or calibration problems.

In order to separate these effects, we have made a series of joint spectral fits of *ROSAT* PSPC, *ASCA* GIS, and *ASCA* SIS spectra from two fields of the sky, where sufficient amount of blank-sky data exist after thorough screening. Because of the limited data meeting the criteria, the work presented in this paper is not intended to determine the current best estimate of the global CXRB spectrum, but rather a comparison of measurements among *ASCA* and *ROSAT* instruments in the same parts of the sky with consistent modelings.

In Sect. 2, we describe the *ASCA* and *ROSAT* data used in the analysis. Joint spectral fits are described in Sect. 3. The results are discussed in Sect. 4.

2. Observations

2.1. Field selection

The fields have been selected from blank sky fields with both *ASCA* and *ROSAT* observations. Severe screening criteria have been applied to the *ROSAT* data in order to minimize contamination from non-cosmic background. This limits the number of usable fields for our purpose. The fields used for this work, with sufficient amount of screened data, are the Lockman Hole (hereafter LH) and the Lynx-3A (hereafter LX) field. In order to use the same sky fields as much as possible for all instruments, we have selected the PSPC and GIS data from the sky area approximately corresponding to the *ASCA* SIS FOV ($22' \times 22'$). The log of *ROSAT* and *ASCA* observations on these fields are shown in Table 1.

2.2. ASCA observation

The screenings of the *ASCA* data have been made with the following criteria: avoid SAA; earth elevation angle > 5 deg

Send offprint requests to: T. Miyaji (tmiyaji@aip.de)

LETTER

Table 1. Log of *ASCA* and *ROSAT* observations

	Lockman Hole (LH)	Lynx-3A (LX)
ASCA observations		
Pointing(s) (α, δ)	(162.96,57.35)	(132.26,44.83)
(degrees,J2000)	(163.00,57.37)	
Dates obs.	22-24 May 93	13–15 May 93
Obs. Modes	GIS:PH; SIS:4CCD Faint/Bright	
Exp. [s] (GIS/SIS)	55352./47236.	75476./68598.
ROSAT observations		
Seq.	900029p-4	900009p
Dates obs.	26 Apr.-9 May 93	5-6 Apr. 91
Exp. [s]	29588, 8181(PI<52)	23438
Area [min^2]	593.	520.

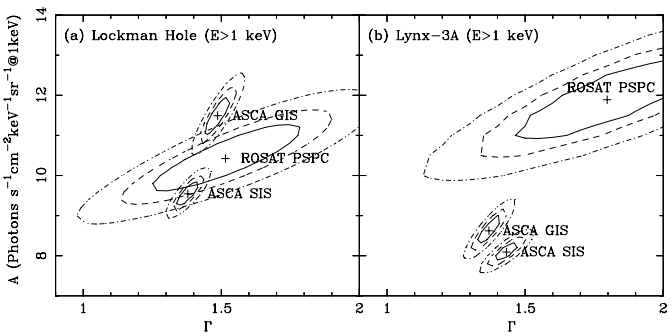

Fig. 1. The confidence contours for single power-law fits to the $E >$ 1 keV data for the three instruments are shown for the LH (a) and LX (b) observations. The contours corresponding to $\Delta\chi^2 = 2.3$, 4.6, and 9.2 from the best-fit values are plotted

(from night earth) or >25 deg (from day earth); avoid 2 minutes after the satellite day-night transition; magnetic cutoff rigidity $>$ 8 GeV/c. The events from hot and flickering pixels of SISs have been removed. The data were taken when the GIS SP-discriminator was disabled, resulting in a high GIS background. Non-cosmic background (NXB) has been collected from night earth observations with the same magnetic cutoff rigidity screening, with 110,300 and 102,066 seconds of exposure for SIS and GIS respectively. The reproducibility of the GIS NXB is about 3% (Ishisaki 1997) and the NXB constitutes about 10% and 30% of the total count for SIS and GIS respectively.

We have created spectral response matrices using a ray-tracing assuming a uniform sky over a large field, taking into account the energy-dependent PSF and stray light problems of the *ASCA* instruments. For the GIS, Ishisaki (1997) estimates the systematic error of the absolute flux measurements using this procedure at $\approx 10\%$.

2.3. ROSAT observation

In this work, we have used the time intervals with the sun-satellite-zenith angle greater than 120 deg (night time, avoiding contaminations by solar scattered X-rays), the geographic latitude between -30 and 30 degrees (tropic), and the Master-Veto (MV) rate between 40 and 170 (the particle background rate can be estimated using the Plucinsky et al. [1997] model). The model particle background (PBG) rates are about 5% of the total events in channels 100<PI<200 (1-2 keV) and 1-2% in 52<PI<99 (0.5–1 keV). Thus possible errors associated with the particle background modeling

does not affect our analysis significantly.

Light curves for the screened data have been further examined to exclude the time range with flux enhancements. In particular, the light curve of low energy channels ($E \leq 0.5$ keV or PI$\leq$51) for LH data show significant variation due to the Long Term Enhancements (LTE)(e.g. Snowden et al. 1994), while no significant light curve variation has been detected for PI$\geq$51. Thus we have used the data from the period where the light curve is close to minimum for the LH PI$\leq$51 spectrum. Since the light curve minimum for a particular pointed observation does not necessarily mean no LTE contamination, limiting our analysis. The EXSAS (Zimmermann et al. 1995) package has been used for data screening, particle background subtraction, and spectrum preparation.

3. Joint spectral fits

3.1. Single power-law fits to $E > 1$ keV data

We have used XSPEC for spectral analysis. The *BBXRT* and *ASCA* results (Sect. 1) show that the CXRB spectrum between 1–10 keV can be well-fitted with a single power-law with $\Gamma \approx 1.4$. Thus we first made single power-law fits to the $E > 1$ keV data as a simple check for consistency among instruments. The PSPC, GIS and SIS pulse height spectra for $E > 1$ keV (PSPC:1.0-2. keV, GIS:1.0–10. keV, SIS:1.0-7. keV) have been fitted with a model of the form $P(E) = AE^{-\Gamma}$, where $P(E)$ is the photon intensity in units of $[\mathrm{photons\,cm^{-2}s^{-1}keV^{-1}sr^{-1}}]$ and E is the photon energy in keV. In the fit, the two parameters, A (normalization) and Γ (photon index) are varied separately or only A is separate while Γ is joined. Fitting results are summarized in Table 2 (fit id. A1–A4) with 90% errors ($\Delta\chi^2 = 2.7$). In A1–A4, all free parameters were varied during the error search.

Confidence contours in the $\Gamma - A$ space, considering statistical errors only, for A1 and A3 are shown in Fig. 1. The disagreements among instruments in Fig. 1 show the level of systematic errors. Possible sources of these systematic errors are discussed in Sect. 4. Adding an $E < 1$ keV excess component to the model did not change the results significantly.

3.2. Broad-band fits (0.1–10 keV)

We have made joint fits to the overall *ROSAT* – *ASCA* spectra over the 0.1 – 10 keV range (0.1-2 keV with PSPC; 0.7–10 keV with GIS and 0.7-7 keV with SIS) considering the following components: (1) an extragalactic power-law component with parameters A and Γ (see above); (2) the hard thermal component, probably associated with the Galactic halo, with plasma temperature $kT^{\rm h}$[keV] and normalization $EI^{\rm h}$ in the XSPEC convention (per steradian); (3) the soft thermal component, from the Local Bubble with $kT^{\rm s}$ and $EI^{\rm s}$. Components (1) and (2)

Table 2. Results of the spectral fits (see text for model and parameter definitions)

Id.	Field	Best-fit parameters[a] (with 90% errors or an asterisk for fixed parameters)	χ^2/ d.o.f
A1	LH	$\Gamma_{\rm P}$=1.5±0.3;$A_{\rm P}$=10.4±0.9; $\Gamma_{\rm G}$=1.49±0.05;$A_{\rm G}$=11.5±0.6; $\Gamma_{\rm S}$=1.38±0.04;$A_{\rm S}$=10.3±0.5	1.04 (258./248)
A2	LH	Γ=1.43±0.04; $A_{\rm P}$=10.3±0.5; $A_{\rm G}$=11.1±0.4; $A_{\rm S}$=9.9±0.4	1.06 (265./250)
A3	LX	$\Gamma_{\rm P}$=1.8±0.4;$A_{\rm P}$=11.9±1.1; $\Gamma_{\rm G}$=1.37±0.05;$A_{\rm G}$=8.6±0.4; $\Gamma_{\rm S}$=1.43±0.04;$A_{\rm S}$=8.1±0.3	1.08 (210./195)
A4	LX	Γ=1.40±0.04; $A_{\rm P}$=10.9±0.6; $A_{\rm G}$=8.9±0.4; $A_{\rm S}$=7.9±0.3	1.09 (215./197)
B1	LH	$N_{\rm H20}=0.56*$;$\Gamma=1.42\pm.03$;$A_{\rm P}=10.0\pm.5$; $kT^{\rm h}=0.142^{+.007}_{-.004}$; $EI^{\rm h}_{\rm P}=18.8\pm1.3$; $kT^{\rm s}=(5.7\pm.9)\times10^{-2}$; $EI^{\rm s}_{\rm P}=9.0^{+2.5}_{-1.4}$; $N_{\rm G}=1.09\pm.05$;$N_{\rm S}=0.96\pm.04$	0.97 (321./332)
B2	LX	$N_{\rm H20}=2.75*$;$\Gamma=1.42\pm.03$;$A_{\rm P}=11.5\pm.7$; $kT^{\rm h}=.148\pm.005$;$EI^{\rm h}_{\rm P}=19.9\pm1.6$; $kT^{\rm s}=(9.0\pm.8)\times10^{-2}$;$EI^{\rm h}_{\rm P}=8.1\pm.3$; $N_{\rm G}=0.81\pm.04$;$N_{\rm S}=0.72\pm.03$	1.06 (351./331)

[a] Subscripts to parameters P:PSPC, G:GIS, S:SIS, none:joint for all instruments.

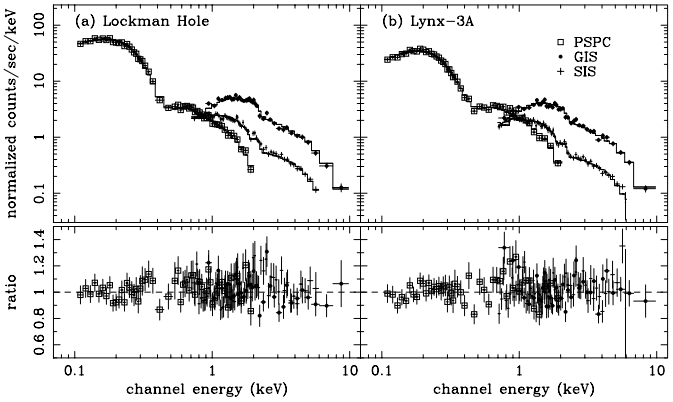

Fig. 2. The 0.1–10 keV pulse-height spectral data with 1σ errors, (appropriately rebinned for display), best-fit models, and the data/model ratio are shown for LH (a) (model B1) and LX (b) (B2). The data are marked according to the instrument as labeled

are absorbed by the interstellar gas with a hydrogen column density fixed to Galactic values ($N_{\rm H20}=0.56[LH];2.75[LX]$ [$10^{20}{\rm cm}^{-2}$], Dicky & Lockman 1990). For components (2) and (3), a Raymond & Smith plasma (distributed as a part of XSPEC), with the solar abundance was assumed. Spectral shape parameters and ratios of normalizations of different spectral components have been joined for all instruments. The overall normalizations have been allowed to vary separately represented by a parameter $N_{\rm G}$ or $N_{\rm S}$, which is the relative normalization to the PSPC value. The pulse height spectra and models are shown in Fig. 2 and fixed/best-fit parameters are listed in Table.2 (B1, B2). The 90% error in Table.2 are formal statistical errors, which have been derived with Γ and temperatures fixed at nominal values while all the normalizations are fitted.

The good fits with the thermal components in the PSPC $E<0.3$ keV data show that the after-pulse (AP) events can be neglected in these observations. Since the *ROSAT* spectra of resolved X-ray sources, mostly extragalactic, are steeper ($\Gamma\approx2.0$, e.g. Hasinger et al. 1993) and a larger flux than inferred from a single power-law fit has already been resolved at $E\sim0.5$ keV, we expect a turn up of the extragalactic component below $E=1$ keV, where the hard thermal component also start to emerge. We could also obtain satisfactory fits with a model where the extragalactic component has a break below 1 keV (fixed to $\Gamma=2.0$ at $E<1$ keV) with the main modification of the hard thermal component normalization (χ^2/ν=0.98 and 1.08 for LH and LX respectively). We could not find satisfactory fits with no hard thermal component but with an extragalactic component excess below 1 keV (either by a broken power-law or an addition of a steeper power-law component). This is because of a clear oxygen line feature around 0.5–0.6 keV in the PSPC spectrum (see also Hasinger 1992).

4. Discussion

There is a bright variable source in LH with [1.2±.2] and [2.5±.7] $\times10^{-13}[{\rm erg\,cm^{-2}\,s^{-1}}]$ for the 0.7-2 keV and 2-7 keV bands respectively (Ogasaka 1997), consisting about 10% of the total ASCA fluxes in both bands. This source was much fainter during the PSPC observation. Thus one should decrease the GIS and SIS normalizations about 10% lower when comparing with the PSPC data. In this case, the agreement between PSPC and GIS is excellent and falls well within statistical errors of each other. For both LH and LX, the SIS data consistently show $\approx10\%$ lower normalizations compared to GIS. This might be caused by incomplete calibration for the radiation damage of the SIS with the 4CCD mode, which can even exist at this level after a few months after the launch, when LH and LX were observed (Dotani et al. 1995).

In the LX observation, a larger discrepancy exists. The GIS and SIS normalizations are lower than the PSPC value by $\approx20\%$ and $\approx30\%$ respectively and slopes are shallower. The ASCA LX normalizations are also significantly lower than those of LH. There is no variable source which can cause this amount of discrepancy in LX. The fact that the 0.1–10 keV fit still show the disagreement of the normalization (see $N_{\rm G}$ in B2) shows that this is not a modeling problem (e.g. leak of the $E>1$ keV excess with the PSPC energy resolution). One possible explanation is the LTE (e.g Snowden et al. 1994), which is usually apparent in the $E<0.5$ keV channels of the PSPC data, but sometimes extends above 1 keV when the activity is high. There may also be an over-subtraction of the NXB background from the *ASCA* data. Furthermore, the instruments are not looking at exactly the same part of the sky. Due to the stray-light and PSF of the

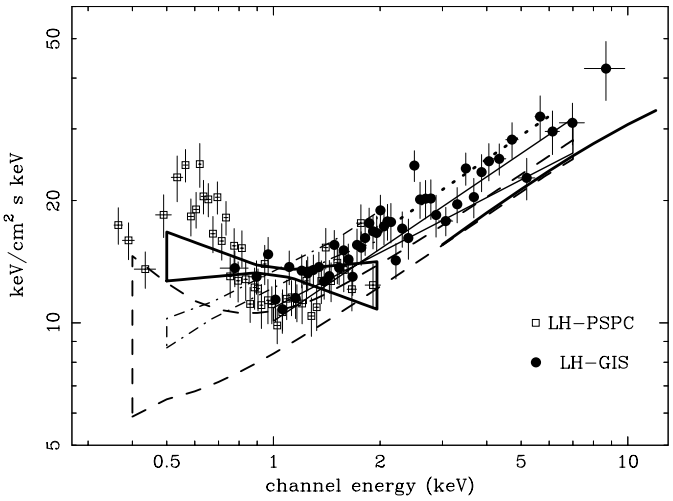

Fig. 3. The PSPC and GIS $E\,I(E)$ spectra (using a two power-law model as an appropriate smooth function for unfolding purpose) of LH are shown and compared with previous measurements: the thick solid bowtie is from Hasinger (1992); the dot-dashed bowtie from Georgantopoulos et al. (1996), both used *ROSAT* PSPC. The dotted line is from rocket measurements (McCammon & Sanders 1990). The long-dashed horn is from an *ASCA* SIS measurement by Gendreau et al. 1995 and the thin solid bowtie is a joint *ROSAT* PSPC/*ASCA* SIS analysis of QSF3 by Chen et al. (1997) for $E > 1$ keV. The thick solid line represents the HEAO-1 A2 measurement by Marshall et al. (1980)

ASCA instruments, $\approx 40\%$ of the GIS/SIS flux comes from outside of the designated FOV (estimated using our ray-tracing program). These effect may also contribute to this discrepancy.

The best consistency for a certain region of the sky from this work is seen for the PSPC and GIS data on LH. Thus it is instructive to compare the observed spectra of these with previous CXRB measurements. The comparison is shown in Fig. 3. Fig. 3 shows a large excess at $E \sim 0.6$ keV on the PSPC data, inconsistent with Gendreau et al.'s *ASCA* SIS data. This may be partially due to the low Galactic column density of LH. The LH GIS data for $E \gtrsim 2$ keV are above the HEAO-1 A2 and Gendreau et al. (1995) SIS values. We note, however, that about 10% of source fluctuation is expected over this small area. Since the ASCA LH data contains a bright source ($\sim 5 \times 10^{-13}$erg s^{-1} cm^{-2} in 2–10 keV), this field should be one of the brighter ones. We also note, however, that an integration from the brightest source in the field to the faintest source excluded in the collimator experiments (e.g. $\approx 2 \times 10^{-11}$erg s^{-1} cm^{-2} in 2–10 keV for HEAO-1 A2 measurement by Marshall et al. 1980) would add $\approx 10\%$ of intensity. A thorough treatment of source fluctuations using a larger area and comparing spectra with appropriate source removal will be presented in a future paper.

In summary, a close look at *ROSAT* and *ASCA* spectra for the same regions of the sky have revealed systematic errors caused by response calibration problems and non cosmic background subtraction of up to $\approx 20 - 30\%$ for one set of observations. These probably caused the reported disagreements between *ASCA* and *ROSAT* measurements (Hasinger 1996), while modelings and sky selection can also contribute. We have obtained a fair description of the CXRB spectrum over 0.1–10 keV range cosisting of a extragalactic power-law component (either single or broken below 1 keV), hard and soft thermal components with a satisfactory fit to all instruments.

Acknowledgements. TM was supported by a fellowship from the Max-Planck Society during his appointment at MPE. This work is partially supported by the Japanese-German collaboration on X-ray astronomy sponsored by JSPS and MPE.

References

Boldt E., 1987, Physics Reports 146, 215
Chen L.-W., Fabian A.C., Gendreau K.C., 1997, MNRAS 285, 499
Dicky J.M., Lockman F.J., 1990 ARAA 28, 215
Dotani T., Yamashita A., Ramussen A. et al., 1995 ASCA News 3, 25
Gendreau K.C., Mushotzky R.F., Fabian A.C. et al., 1995, PASJ 47, L5
Georgantopoulos I., Stewart G., Shanks T., et al., 1996, MNRAS 280, 276
Hasinger G., 1992 in The X-ray Background, eds. X. Barcons, A.C. Fabian, (Cambridge U. Press: Cambridge), 299
Hasinger G., Burg R., Giacconi R., et al., 1993, A&A 275, 1
Hasinger G., 1996 A&AS, 120, C607
Ishisaki Y., 1997 Ph.D. thesis, University of Tokyo
Ishisaki Y. et al., 1998 ApJL, submitted
Jahoda K. et al., 1992 in The X-ray Background, eds. X. Barcons, A.C. Fabian, (Cambridge U. Press: Cambridge), 240
McCammon D., Sanders W.T., 1990, ARAA 28, 657
Marshall F.E., Boldt E.A., Holt S.S. et al., 1980, ApJ 235, 4
Ogasaka, Y., 1997 Ph.D. thesis, Gakushuin University
Plucinsky P.P., Snowden S.L., Briel U.G., Hasinger G., Pfeffermann E., 1993, ApJ 418, 519
Snowden, S.L., McCammon D., Burrows D.N., Mendenhall, D.N., 1994 ApJ 424, 714
Zimmermann H.U., Becker W., Belloni T. et al., 1994, EXSAS User's Guide, MPE Report 257, (Garching:MPE)